The Cell's Biological Rods and Ropes

David Boal

Introduction

Despite a variety of shapes and sizes, the generic mechanical structure of cells is remarkably similar from one cell type to the next.[1] All cells are bounded by a plasma membrane, a fluid sheet that controls the passage of materials into and out of the cell. Plant cells and bacteria reinforce this membrane with a cell wall, permitting the cell to operate at an elevated osmotic pressure. Simple cells, such as the bacterium shown in Figure 1a, possess a fairly homogeneous interior containing the cell's genetic blueprint and protein workhorses, but no mechanical elements. In contrast, as can be seen in Figure 1b, plant and animal cells contain internal compartments and a filamentous cytoskeleton—a network of biological ropes, cables, and poles that helps maintain the cell's shape and organize its contents.

Four principal types of filaments are found in the cytoskeleton: spectrin, actin, microtubules, and a family of intermediate filaments. Not all filaments are present in all cells. The chemical composition of the filaments shows only limited variation from one cell to another, even in organisms as diverse as humans and yeasts. Membranes have a more variable composition, consisting of a bilayer of dual-chain lipid molecules in which are embedded various proteins and frequently a moderate concentration of cholesterol. The similarity of the cell's mechanical elements in chemical composition and physical characteristics encourages us to search for universal strategies that have developed in nature for the engineering specifications of the cell. In this article, we concentrate on the cytoskeleton and its filaments.

To understand how biopolymers function within a network, we review in the next section the elastic properties of filaments in isolation. The following sections explore two-dimensional (2D) networks of permanently welded filaments and three-dimensional (3D) networks of permanent and nonpermanent cross-links, where we summarize several theoretical results from spring networks that are useful for interpreting biological systems. In the final section, we apply our knowledge of these networks to a particularly simple cell: the human red blood cell.

Polymers

In most cells, the cytoskeleton contains at least two of the four principal protein filaments:

- *Spectrin* is a single polymer with rigid barrel-like sections linked by a thin string, like pearls on a necklace. The barrels arise from attractive interactions between monomers, causing the string to fold back on itself like a Z.
- *Actin* is a polymer of polymers. Actin monomers, themselves a folded polymer of amino acids, assemble into a protein rope called F-actin (F for filamentous), having the superficial appearance of two strands forming a coil.
- *Intermediate filaments* have a complex hierarchical structure. Thirty-two individual protein strands are intertwined and bundled to form a hollow cylinder.
- *Microtubules* are composed of tubulin, which comes in two varieties that can form a heterodimer. The dimers can assemble end-to-end successively into linear protofilaments, 13 of which form a hollow microtubule (in most cells).

The approximate diameters of the filaments range from 8 nm (actin) to 25 nm (microtubules), and their mass per unit length varies by more than a factor of 10, as summarized in Table I.

In thermal equilibrium, flexible filaments do not adopt a unique shape; rather, they bend and twist as they exchange energy with their surroundings. Consider the extreme situation in which the filament is a chain of N identical segments of length b connected at unrestricted pivots, as illustrated in Figure 2.

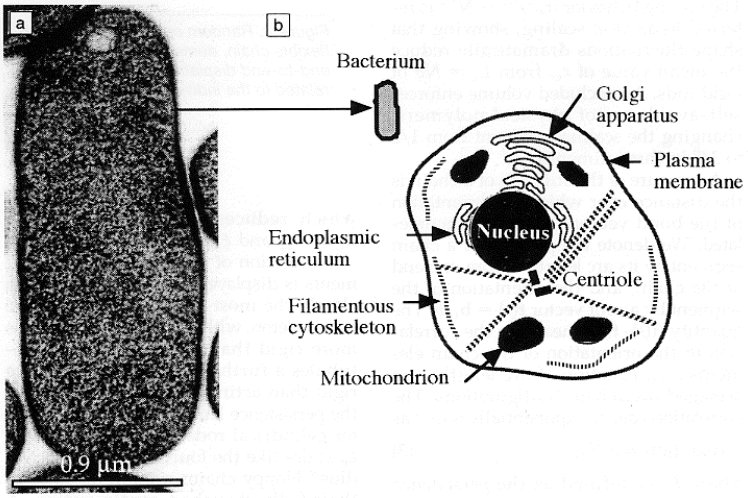

Figure 1. (a) A thin section of the bacterium Escherichia coli, *which is bounded by a complex cell wall but has little internal structure (courtesy of Terry Beveridge). (b) Layout of a generic animal cell, showing structural elements such as the plasma membrane and the cytoskeleton as well as a selection of organelles (nucleus, endoplasmic reticulum, mitochondrion, and Golgi apparatus). The bacterium from (a) is reproduced in (b) to show its relative size.*

Table I: Approximate Diameter, Linear Density (Mass Per Unit Length), and Persistence Length of Some Biologically Important Polymers.

Polymer	Diameter (nm)	Linear density (Da/nm)	Persistence length (nm)
Long alkanes	0.2	~110	~0.5
Spectrin (2 strands)	...	4,600	10–20
DNA (2 strands)	1	1,900	53 ± 2
F-actin	~8	16,000	$10–20 \times 10^3$
Intermediate filaments	~10	~35,000	...
Tobacco mosaic virus	18	~140,000	$\sim 1 \times 10^6$
Microtubules	25	160,000	$2–6 \times 10^6$

Representing the length and orientation of each segment by a vector $\mathbf{b}_i$, the contour length of the chain is $L_c = Nb$, and the end-to-end displacement vector is

$$\mathbf{r}_{ee} = \sum_{i=1}^{N} \mathbf{b}_i . \qquad (1)$$

The ensemble average of $\mathbf{r}_{ee}^2$ over all chains with the same N is $\langle \mathbf{r}_{ee}^2 \rangle = \Sigma_i \Sigma_j \langle \mathbf{b}_i \cdot \mathbf{b}_j \rangle$. In a random chain, the orientation of any pair of bonds is independent, such that the ensemble average of $\mathbf{b}_i \cdot \mathbf{b}_j$ vanishes for $i \neq j$. Each of the diagonal terms ($i = j$) equals b^2, so that

$$\langle \mathbf{r}_{ee}^2 \rangle = Nb^2 \qquad \text{(random chain)}. \qquad (2)$$

The scaling behavior $\langle \mathbf{r}_{ee}^2 \rangle^{1/2} \sim N^{1/2}$ is referred to as *ideal* scaling, showing that shape fluctuations dramatically reduce the mean value of r_{ee} from $L_c = Nb$ of rigid rods. An excluded volume enforces self-avoidance of physical polymers, changing the scaling exponent from 1/2 to 3/5 in three dimensions.[2]

A measure of the stiffness of a chain is the distance over which the orientation of the bond vectors becomes uncorrelated. We denote the position of a chain segment by its arc length s from one end of the chain, and the orientation of the segment by a unit vector $\mathbf{t}(s) = \mathbf{b}_i/b$. The quantity $\langle \mathbf{t}(s) \cdot \mathbf{t}(0) \rangle$ measures the correlation in the orientation of the chain elements as a function of arc length s, as averaged over chain configurations. The correlations decay exponentially with s as

$$\langle \mathbf{t}(s) \cdot \mathbf{t}(0) \rangle = e^{-s/\xi_p}, \qquad (3)$$

where ξ_p is defined as the *persistence length*. A small persistence length implies that the chain is floppy and changes direction rapidly with increasing s. The end-to-end displacement is related to ξ_p by[3]

$$\langle \mathbf{r}_{ee}^2 \rangle = 2\xi_p L_c - 2\xi_p^2 (1 - e^{-L_c/\xi_p}), \qquad (4)$$

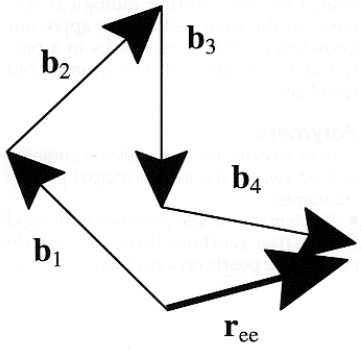

Figure 2. Random configuration of a flexible chain, demonstrating how the end-to-end displacement vector $\mathbf{r}_{ee}$ is related to the individual bond vectors.

which reduces to Equation 2 when $L_c >> \xi_p$ and $\xi_p = b/2$.

A selection of results for protein filaments is displayed in Table I. Spectrin is clearly the most flexible element of the cytoskeleton, with actin a thousand times more rigid than spectrin, and microtubules a further thousand times more rigid than actin. This large variation in the persistence length is not unexpected: for cylindrical rods of constant density, ξ_p scales like the fourth power of the radius.[4] Floppy chains are rarely found in their fully stretched configuration: A chain can sample a much larger number of convoluted configurations than highly stretched ones. Proportional to the logarithm of the number of configurations, the entropy of a chain is reduced, and its free energy increased, as the chain is stretched. This implies that a floppy chain has elasticity by virtue of its entropy, behaving like a spring with spring constant

$$k_{sp} = \frac{3k_B T}{Nb^2} \qquad \text{(ideal chains)} \qquad (5)$$

in three dimensions. Equation 5 demonstrates that the effective stiffness of the chain increases with the temperature.

Two-Dimensional Networks

The membrane-associated cytoskeleton of the human red blood cell is a prime example of a 2D biological network. Composed of spectrin tetramers, the erythrocyte cytoskeleton is highly convoluted *in vivo*, but can be stretched by about a factor of seven in area to reveal its relatively uniform four- to sixfold connectivity,[5] as shown in Figure 3a. The tetramers are attached to one another at junction complexes with an average separation *in vivo* of about 75 nm, much shorter than their contour length of 200 nm. An example of a 2D biological network with fourfold symmetry is the lateral cortex of the auditory outer hair cell, consisting of inequivalent filaments (thought to be spectrin and actin) joined at right angles.[6]

To describe the mechanics of these networks, we briefly recall a few results from the theory of elasticity. Under deformation, the change in position of a given element of an object is represented by a displacement vector $\mathbf{u}$, which varies locally on the object. The energetics of the deformation lies in the strain tensor u_{ij}, which is related to the rate of change of $\mathbf{u}$ with position $\mathbf{x}$ by $u_{ij} \cong 1/2[\partial u_i/\partial x_j + \partial u_j/\partial x_i]$ for small deformations. In Hooke's law materials, the change in the free-energy density $\Delta\mathcal{F}$ upon deformation is quadratic in u_{ij}, and has the form[4]

$$\Delta\mathcal{F} = \frac{K_A}{2}(u_{xx} + u_{yy})^2 + \mu\left\{\frac{(u_{xx} - u_{yy})^2}{2} + 2u_{xy}^2\right\} \qquad (6)$$

for isotropic materials or triangular networks in two dimensions, where K_A and μ are the area-compression modulus and 2D shear modulus, respectively.

Spring networks show how macroscopic measures of elasticity, such as K_A and μ, can be related to the microscopic properties of a material. Consider a uniform network of springs, with spring constant k_{sp}, connected together at sixfold coordinated junctions to form trian-

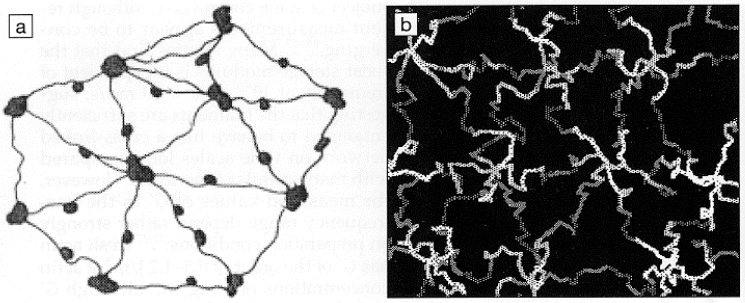

Figure 3. (a) Drawing of a spread erythrocyte cytoskeleton, copied from an electron microscope image (from Reference 5). (b) Computer simulation of the equilibrated cytoskeleton, in which each spectrin tetramer is represented by a single polymer chain, linked at sixfold vertices, and attached at their midpoints to a flat computational bilayer.

gular plaquettes. At low temperatures, this network obeys[7]

$$K_A = \left(\frac{\sqrt{3}\,k_{sp}}{2}\right)\cdot\left(1+\frac{\Pi}{\sqrt{3}\,k_{sp}}\right) \text{ and } \quad (7)$$

$$\mu = \left(\frac{\sqrt{3}\,k_{sp}}{4}\right)\cdot\left(1-\frac{\sqrt{3}\,\Pi}{k_{sp}}\right), \quad (8)$$

when subject to a 2D stress Π, demonstrating that the elastic moduli are proportional to the spring constant. Be aware that not all of the physics of these networks are properly expressed by Equations 7 and 8: The network is observed to collapse when the compressive stress exceeds a certain threshold.[8,9] Other interesting properties predicted for these networks include

- a negative Poisson ratio under a certain range of tensile stress, meaning that the network expands laterally when stretched longitudinally; and
- a negative coefficient of thermal expansion at low temperatures.[10]

A qualitative expression for the shear modulus (or compression modulus) of floppy chains can be obtained from Equation 8, which states that $\mu \sim k_{sp}$. We saw earlier that ideal chains behave like springs, with an effective spring constant given by Equation 5, namely, $k_{sp} \sim k_B T/Nb^2$. Furthermore, the linear size of a single polymer is roughly $(Nb^2)^{1/2}$, according to Equation 2, so the number of chains per unit area ρ is of the order of $1/Nb^2$. Thus, we expect

$$\mu \sim \rho k_B T \quad \text{(ideal chains)}. \quad (9)$$

A somewhat more rigorous, but still not exact, treatment of ideal chains[11,12] also yields Equation 9. We now apply the concept of entropic elasticity to a particularly simple cytoskeleton.

As measured by micromechanical manipulation,[13] the shear modulus of the human erythrocyte is $6–9 \times 10^{-6}$ J/m^2, although measurements based upon thermal fluctuations[14] give lower values for μ. Regarded as a network of ideal polymers,[15] the spectrin network of the red blood cell would be expected to have $\mu \sim 3 \times 10^{-6}$ J/m^2 from Equation 9, within a factor of two of experiment. However, we should not be misled into believing that all aspects of cytoskeleton elasticity are entropic. The auditory outer hair cell has a 2D cortex with a filament density somewhat higher than the erythrocyte, but a measured[16] shear modulus a thousandfold larger than the nominal value of $\rho k_B T$. The cortex includes actin, which is stiff on small length scales and should make an energetic contribution to the elasticity.

Three-Dimensional Networks

Actin, intermediate filaments, and microtubules, in isolation or together, form a variety of 3D networks. In some cells, specific proteins bind the filaments together with some degree of permanence, while in others, the filaments may be entangled, but not permanently cross-linked. How do we represent the elastic properties of 3D networks? For isotropic systems, the change in the free-energy density associated with deformation has a similar form to Equation 6,

$$\Delta\mathcal{F} = \left(\frac{K_V}{2}\right)(u_{trace})^2 + \mu\sum_{i,j}\left(u_{ij} - \frac{\delta_{ij}u_{trace}}{3}\right)^2 \quad (10)$$

where the two elastic parameters are the volume compression modulus K_V and the 3D shear modulus μ. Our theoretical toolkit for these moduli includes the approximate relation[11,12] $\mu \sim \rho k_B T$, which applies to cross-linked networks, entangled networks (at intermediate time scales), and rigid rods (at short time scales), where ρ is now the effective number of filaments per unit volume.

Solutions of polymers without cross-links must behave like fluids when observed over long time scales: The polymers can wiggle past each other due to thermal motion as the system deforms in response to an applied shear. However, on short time scales, the network may offer resistance to an applied strain or stress, a behavior referred to as viscoelasticity. As illustrated in Figure 4, poly-

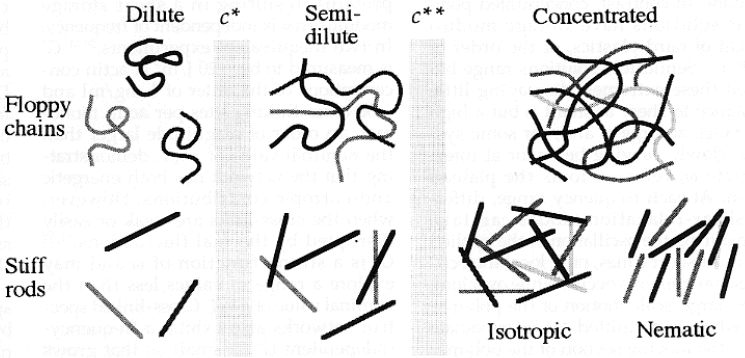

Figure 4. Generic behavior of polymer solutions as a function of filament concentration, which increases from left to right; $c^* \sim L_c^{-3}$, $c^{**} \sim (DL_c^2)^{-1}$.

mer solutions can be classified into several concentration regimes, each with different viscoelastic characteristics.[3] Consider a solution of stiff rods of length L_c and diameter D. In the dilute regime at concentrations below $c^* \sim L_c^{-3}$, the rods are sufficiently separated in space that the solution's viscosity is close to that of its solvent. At the other extreme, the filaments strongly overlap and intertwine in the concentration regime above $c^{**} \sim (DL_c^2)^{-1}$, forming isotropic or nematic phases, the latter having long-range orientational order. Between c^* and c^{**} lies the semidilute regime, characteristic of many biopolymer solutions.

How do we formally describe a material whose response to an imposed stress or strain is time-dependent? Commonly, the frequency-dependence of the elastic response is measured by subjecting the material to an oscillating strain of the form $u_{xy}(t) = u^0_{xy} \sin\omega t$, where u^0_{xy} is the amplitude of the strain and ω is its frequency. The stress/strain relationship for this situation has the form[17]

$$\sigma_{xy} = u^0_{xy} G'(\omega) \sin\omega t + u^0_{xy} G''(\omega) \cos\omega t, \quad (11)$$

where σ_{xy} is the shear stress. The functions $G'(\omega)$ and $G''(\omega)$ are called the shear storage and shear loss moduli, respectively, and are measures of the energy stored (and recovered) or lost during a cycle of the system. As ω vanishes, G' and G''/ω become the shear modulus and viscosity, respectively; for true fluids, G' should vanish at $\omega = 0$.

The behavior of the storage modulus as a function of frequency depends upon the nature of the viscoelastic material, as illustrated in Figure 5. Dilute solutions display the smallest storage moduli, as might be expected from their near-fluid behavior. In contrast, concentrated polymeric solutions have storage moduli typical of hard plastics, of the order of 10^9 J/m^3. Semidilute solutions range between these extremes, displaying little resistance to shear at small ω but a high resistance at large ω and, for some systems, slowly varying behavior at intermediate ω, referred to as the plateau region. At each frequency range, different shear-relaxation modes can take place during the oscillation of the applied strain. At short times, only local molecular rearrangements occur, while over long times, large-scale motion of the polymer as a whole is permitted. At intermediate times, the moving section of the polymer may have a length comparable to the distance between entanglement points, which behave like fixed, if transient, cross-links.

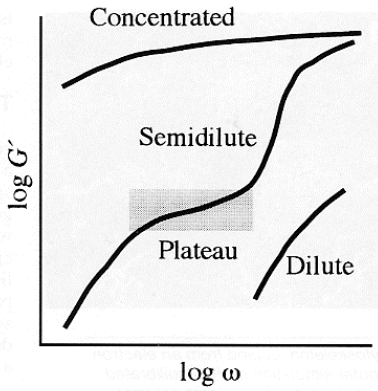

Figure 5. Schematic representation of the storage modulus G′(ω) as a function of frequency ω for three sample concentrations: dilute, semidilute, and concentrated.

We now turn to experimental measurements of biofilament solutions with and without permanent cross-links. Several types of filaments have been purified and reconstituted into networks whose properties can be studied under a broader range of conditions than are found in a cellular environment. Alternatively, networks can be probed in the cells themselves, for instance, by injecting fluorescent markers that allow the local response of the cytoskeleton to be imaged. We consider only reconstituted networks here; guides to recent work on cellular networks can be found in References 18 and 19.

Actin filaments can be permanently cross-linked by several actin-binding proteins, resulting in a shear storage modulus that is independent of frequency. In two inequivalent experiments,[20,21] G' is measured to be ~20 J/m^3 at actin concentrations of the order of 1 mg/ml and ~50 cross-linking sites per actin monomer, an order of magnitude larger than the nominal value of $\rho k_B T$, demonstrating that the network has both energetic and entropic contributions. However, when the cross-links are weak or easily disrupted by thermal fluctuations,[21,22] G' is a strong function of ω and may explore a range of values less than the nominal value of $\rho k_B T$. Cross-linked spectrin networks also exhibit a frequency-independent G' (at small ω) that grows linearly with spectrin concentration.[23]

The behavior of actin networks without permanent cross-links has been the subject of some controversy, although recent measurements appear to be converging.[24–27] Many studies find that the shear storage modulus is independent of frequency at $10^{-3} < \omega < 10$ rad/s, suggesting that the filaments are sufficiently entangled to behave like a cross-linked network on time scales long compared with many cellular time scales. However, the measured values of G' in the low-frequency range depend rather strongly on preparation conditions:[24,27] fresh actin has G' of the order of 0.5–1.2 J/m^3 at actin concentrations of 1 mg/ml, although G' rises by an order of magnitude as the actin ages. However, the behavior of the plateau modulus[24–26] is more subtle than just $\rho k_B T$: G' increases with concentration as $\rho^{1.3-1.4}$. This concentration dependence is in agreement with theoretical expectations[28–30] of semidilute solutions of semiflexible filaments, which predict a scaling of $\rho^{7/5}$. At higher actin concentrations, the filaments adopt a nematic phase (see Reference 31 and references therein).

The viscoelastic behavior of microtubules and vimentin (an intermediate filament) has also been examined.[32] These solutions are observed to be much stiffer than their nominal value of $\rho k_B T$, having G' in the range of 2–3 J/m^3 for filament concentrations of 2 mg/ml, with little frequency dependence. The concentration dependence of G' varies as $c^{1.3}$ for microtubules and $c^{0.5}$ for vimentin; the scaling of the microtubules is not very far from that of rigid rods, but the weak concentration dependence of vimentin solutions is not understood.

The Whole Cell

We now apply our understanding of flexible networks to one of the mechanically simplest cells with a cytoskeleton, mammalian red blood cells, which derive their shear resistance from the membrane-associated cytoskeleton consisting predominantly of spectrin tetramers, as described in the section on "Two-Dimensional Networks." The energetics for many deformations of interest here originate in the cytoskeleton, and the bending energy of the membrane is not a significant contributor. The fact that the interjunction spacing is so much less than the contour length of the tetramers suggests that the elasticity of this cytoskeleton is of entropic origin.[15]

Many of the elastic properties of the spectrin cytoskeleton can be captured[33] by representing it as a quasi-2D polymer network, as in Figure 3b, having of the order of 20 polymer segments per spectrin tetramer. This is computationally viable for a membrane patch, but pro-

hibitive for a whole cell. Replacing the chains by effective two- and three-body interactions between network nodes[34] permits the simulation of whole cells, as demonstrated in Figure 6. Figure 6a is a bright-field microscope image of an osmotically swollen red blood cell as it is drawn up a micropipet by suction.[35] Figure 6b is an image of the density of the membrane-associated cytoskeleton, to which fluorescent molecules have been attached, showing how the cytoskeleton becomes ever more dilute, and hence less visible in the image, as it is stretched up the micropipet.[35] Figure 6c is a computer simulation,[34] which does a reasonable job of reproducing the observed response of the cytoskeleton, with suitable choice of network conditions.

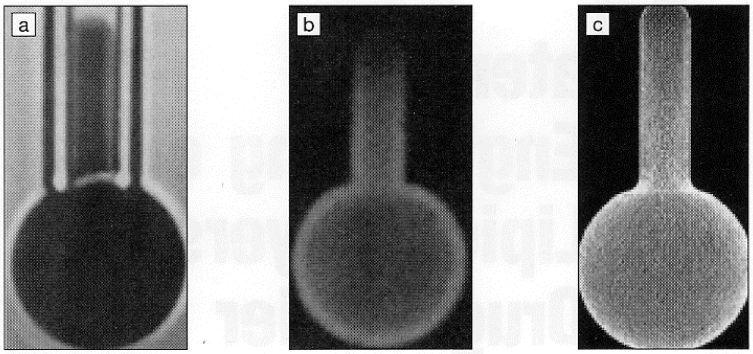

Figure 6. Deformation of a human red blood cell as it is drawn up a micropipet approximately 1 μm in diameter. (a) A bright-field microscope image of the cell and the pipet, and (b) a fluorescent image showing the density of the cytoskeleton.[35] (c) A computer simulation of the same type of deformation.[34]

Summary

The mechanical rigidity of cells is provided by networks and mats of filamentous proteins and other compounds which form the cell wall and cytoskeleton. These materials span an enormous range of deformation resistance: Networks of actin at physiological concentrations have a compression resistance several orders of magnitude *less* than the air we breathe, while a thin layer of peptidoglycan permits some bacteria to operate at pressures of the order of 20 atm. The elastic properties of these soft materials have both energetic and entropic origins, and their theoretical treatment uses concepts from classical and statistical mechanics.

Although our knowledge of the static and dynamic characteristics of biological materials is incomplete, it is nevertheless sufficiently advanced that quantitative predictions can be made for the behavior of such structurally simple cells as mammalian red blood cells, mycoplasmas, and some bacteria. The list of problems that are likely to be the subject of continuing scrutiny over the coming decade is very long, and would include

- cell dynamics, such as locomotion and division;
- the failure of the bacterial cell wall, induced by antibiotics;
- the formation of simple cells early in the Earth's evolutionary history; and
- the mechanical and electrical interaction between cells and semiconductors.

As this list demonstrates, the joy of working in this field of research is its strong multidisciplinary nature and its wealth of fundamental and applied problems, sure to keep many of us busy for years to come.

Acknowledgments

This work is supported in part by the Natural Sciences and Engineering Research Council of Canada.

References

1. B. Alberts, D. Bray, J. Lewis, M. Raff, K. Roberts, and J.P. Watson, *Molecular Biology of the Cell*, 3rd ed. (Garland, New York, 1994), p. 12.
2. P.J. Flory, *Statistical Mechanics of Chain Molecules* (Wiley, New York, 1969).
3. M. Doi and S.F. Edwards, *The Theory of Polymer Dynamics* (Oxford University Press, Oxford, 1986) p. 316.
4. L.D. Landau and E.M. Lifshitz, *Theory of Elasticity* (Pergamon Press, Oxford, 1986), p. 32.
5. S.-C. Liu, L.H. Derick, and J. Palek, *J. Cell Biol.* **104** (1987) p. 527.
6. M.C. Holley and J.F. Ashmore, *J. Cell Sci.* **96** (1990) p. 283.
7. D.H. Boal, U. Seifert, and J.C. Shillcock, *Phys. Rev. E* **48** (1993) p. 4274.
8. D.E. Discher, D.H. Boal, and S.K. Boey, *Phys. Rev. E* **55** (1997) p. 4762.
9. W. Wintz, R. Everaers, and U. Seifert, *J. Phys. I (France)* **7** (1997) p. 1097.
10. P. Lammert and D.E. Discher, *Phys. Rev. E* **57** (1998) p. 4386.
11. P.J. Flory, *Principles of Polymer Chemistry* (Cornell University Press, Ithaca, NY, 1953), p. 464.
12. R.L.G. Treloar, *The Physics of Rubber Elasticity* (Oxford University Press, Oxford, 1975).
13. R. Waugh and E.A. Evans, *Biophys. J.* **26** (1979) p. 115.
14. H. Strey, M. Peterson, and E. Sackmann, *Biophys. J.* **69** (1995) p. 478.
15. E.A. Evans, *Biophys. J.* **13** (1973) p. 926.
16. P.S. Sit, A.A. Spector, A.J.-C. Lue, A.S. Popel, and W.E. Brownell, *Biophys. J.* **72** (1997) p. 2812.
17. J.D. Ferry, *Viscoelastic Properties of Polymers*, 3rd ed., Chapter 1 (Wiley, New York, 1980).
18. G.K. Ragsdale, J. Phelps, and K. Luby-Phelps, *Biophys. J.* **73** (1997) p. 2798.
19. A.R. Bausch, W. Möller, and E. Sackmann, *Biophys. J.* **76** (1999) p. 573.
20. P.A. Janmey, S. Hvidt, J. Lamb, and T.P. Stossel, *Nature* **345** (1990) p. 89.
21. J. Xu, D. Wirtz, and T.D. Pollard, *J. Biol. Chem.* **273** (1998) p. 9570.
22. M. Sato, W.H. Schwarz, and T.D. Pollard, *Nature* **325** (1987) p. 828.
23. B.T. Stokke, A. Mikkelsen, and A. Elgsaeter, *Biochim. Biophys. Acta* **816** (1985) p. 102.
24. J. Xu, W.H. Schwarz, J.A. Käs, T.P. Stossel, P.A. Janmey, and T.D. Pollard, *Biophys. J.* **74** (1998) p. 2731.
25. B. Hinner, M. Tempel, E. Sackmann, K. Kroy, and E. Frey, *Phys. Rev. Lett.* **81** (1998) p. 2614.
26. A. Palmer, T.G. Mason, J. Xu, S.C. Kuo, and D. Wirtz, *Biophys. J.* **76** (1999) p. 1063.
27. J. Tang, P.A. Janmey, T.P. Stossel, and T. Ito, *Biophys. J.* **76** (1999) p. 2208.
28. H. Isambert and A.C. Maggs, *Macromolecules* **29** (1996) p. 1036.
29. D.C. Morse, *Phys. Rev. E* **58** (1998) p. R1237.
30. F. Gittes and F.C. MacKintosh, *Phys. Rev. E* **58** (1998) p. R1241.
31. R. Furukawa, R. Kundra, and M. Fechheimer, *Biochemistry* **32** (1993) p. 12346.
32. P.A. Janmey, U. Euteneuer, P. Traub, and M. Schliwa, *J. Cell Biol.* **113** (1991) p. 155.
33. D.H. Boal, *Biophys. J.* **67** (1994) p. 521.
34. D.E. Discher, D.H. Boal, and S.K. Boey, *Biophys. J.* **75** (1998) p. 1584.
35. D.E. Discher, N. Mohandas, and E.A. Evans, *Science* **266** (1994) p. 1032. □